

## Flammability limits of an oxidation reaction in a batch reactor. II. The Rychlý mechanism

M.I. Nelson

*School of Mathematics and Applied Statistics, University of Wollongong, Wollongong, NSW2522, Australia*  
E-mail: mnelson@uow.edu.au

H.S. Sidhu

*School of Mathematics and Statistics, Australian Defence Force Academy, University of New South Wales, Canberra 2600, Australia*

Received 9 July 2003

It is often numerically convenient to reduce models in two-dimensions to one-dimension. This can be done formally through the use of centre manifold techniques, or informally using physical reasoning. We investigate the extent to which flammability limits in a two-dimensional slab are accurately represented by the values in the corresponding one-dimensional slab. We use a simple chemical mechanism containing exothermic and endothermic reactions that has been used to model the combustion of hydrocarbon fragments produced by polymer pyrolysis.

**KEY WORDS:** flammability limits

**AMS subject classification:** 80A25

### 1. Introduction

It is well known that premixed flames only exist within certain parameter ranges, or flammability limits, that correspond to a rate of heat production that is sufficient to sustain the reaction [1]. In this work we compare flammability limits calculated from two- and one-dimensional models of a batch reactor. As it is numerically convenient to reduce problems in two-dimensions to one-dimension, the motivation for this work is to determine under which conditions this reduction is valid. Besides our earlier paper [2] we are not aware of any other comparisons between one- and two-dimensional reactors within the context of flammability limits.

In our previous paper the oxidation chemistry was represented by a single one-step global irreversible reaction that is first order with respect to both of the reactants. In this paper we use an extension of this mechanism which has been used to model the combustion of hydrocarbons produced by the pyrolysis of polymers [3–6]. Our aim is to investigate the sensitivity of our previous results to the choice of mechanism.

## 2. Description of the model

The reaction mixture, comprising fuel ( $\mathcal{F}$ ) and oxygen ( $\mathcal{O}_2$ ) is assembled in a batch reactor with a specified total concentration ( $C$ ) and at a designated ambient temperature ( $T_a$ ). The initial concentrations of both fuel and oxygen concentrations are assumed to be spatially uniform and are given by  $\alpha C$  and  $(1 - \alpha)C$ , respectively. In these expressions the parameter  $\alpha$  is referred to as the fuel fraction and is the ratio of the initial fuel concentration to the total reactant concentration:

$$\alpha = \frac{\mathcal{F}(t = 0)}{\mathcal{F}(t = 0) + \mathcal{O}_2(t = 0)}. \quad (1)$$

The batch reactor is treated as a slab and we investigate one- and two-dimensional formulations of our model. In the one-dimensional model we include a term in the temperature equation representing bulk heat loss through convective heat-transfer. The incorporation of this term into the reaction–diffusion equation, rather than as a boundary condition, occurs when a two-dimensional problem is reduced to one dimension by taking an appropriate average. Combustion problems, particularly in the context of wave propagation, in which heat-loss is included in this manner have been investigated recently [7–12]. Alternatively, heat-loss of the form used in this paper is often described as representing a volumetric heat-loss.

The initial temperature distribution is assumed to be non-uniform and is written in the form

$$T(x, 0) = T_a + \mathcal{T} f(x), \quad (2)$$

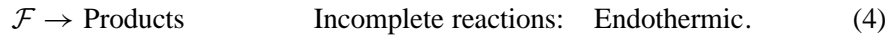
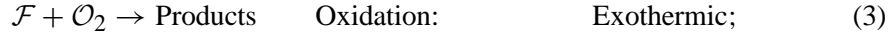
where  $f(x) \geq 0$ ,  $T_a$  is the ambient temperature and we refer to the parameter  $\mathcal{T}$  as the initial condition parameter. We fix the form of the function  $f(x)$  (a Gaussian) and vary the initial condition parameter. This is a simple means for modelling the energy input from an ignition source, viewing the ignition source as a mechanism for changing the initial condition of the system. The Gaussian profile ensures that the energy input decays exponentially away from the local point of initiation.

We investigate the response of the system to changes in the initial condition ( $\mathcal{T}$ ), the fuel fraction ( $\alpha$ ), the effective heat-transfer coefficient ( $\chi \mathcal{G}$ ) and the half-thickness of the two-dimensional slab ( $d$ ). For a given experimental setup the effective heat-transfer coefficient is usually considered fixed although it is possible to vary it. For example, the heat transfer coefficient ( $\chi$ ) can be changed if the batch reactor is placed within a temperature-controlled oven by varying the fan-speed within the oven. Alternatively, the geometric factor  $\mathcal{G}$  may be varied by changing the diameter of the batch reactor.

### 2.1. Model chemistry

The oxidation chemistry is represented by two global irreversible reactions. These represent exothermic oxidation reactions and endothermic “incomplete combustion re-

actions". The former is first order with respect to both of the reactants whereas as the latter is first order with respect to the fuel concentration:



The stoichiometric coefficients are taken to be unitary for simplicity. The global mechanism used in [2] consisted solely of the oxidation step, reaction (3).

### 3. Model equations

In this section we give the governing equations for the mechanism (3), (4) occurring in a slab of nominal length  $2L$  (running from  $x = 0$  to  $x = 2L$ ) and thickness  $2d$  (running from  $y = -d$  to  $y = d$ ). We reduce the integration domain by imposing a symmetry condition along the lines  $x = L$  and  $y = 0$ . The definition of the parameters and the values used in this work are given in table 1.

Table 1  
Parameters and typical parameter values.

$A$	Pre-exponential factor for oxidation	$A = e^{12.6} (\text{m}^3 \text{mol}^{-1} \text{s}^{-1})$
$A_i$	Pre-exponential factor for "incomplete combustion reactions"	$A_i = e^{27.8} (\text{s}^{-1})$
$C$	The concentration of reactants at time $t = 0$	$C = 4 (\text{mol m}^{-3})$
$E$	Activation energy for oxidation	$E = 88 (\text{kJ mol}^{-1})$
$E_i$	Activation energy for "incomplete combustion reactions"	$E = 243 (\text{kJ mol}^{-1})$
$D_f$	Diffusion coefficient of oxygen	$D_f = 5.6 \cdot 10^{-5} (\text{m}^2 \text{s}^{-1})$
$D_o$	Diffusion coefficient of oxygen	$D_f = 5.6 \cdot 10^{-5} (\text{m}^2 \text{s}^{-1})$
$\mathcal{F}$	The concentration of fuel in the reactor	$(\text{mol m}^{-3})$
$\mathcal{G}$	A geometric factor ( $\mathcal{G} = 1/d$ )	$(\text{m}^{-1})$
$L$	Reactor half-length	$L = 0.115 (\text{m})$
$\mathcal{O}_2$	The concentration of oxygen in the reactor	$(\text{mol m}^{-3})$
$Q$	Oxidation exothermicity	$Q = 3000 (\text{kJ mol}^{-1})$
$Q_i$	Modulus of the "incomplete combustion reactions" endothermicity	$Q = 400 (\text{kJ mol}^{-1})$
$R$	Ideal gas constant	$R = 8.31431 (\text{JK}^{-1} \text{mol}^{-1})$
$T$	Temperature	$(\text{K})$
$\mathcal{T}$	Initial condition parameter	$(\text{K})$
$T_a$	Ambient temperature	$T_a = 298 (\text{K})$
$c_v$	Heat capacity of the reaction mixture at constant volume	$c_v = 3R (\text{JK}^{-1} \text{mol}^{-1})$
$d$	Half thickness of the reactor in the $y$ -direction	$(\text{m})$
$k$	Thermal conductivity	$k = 6.0 \cdot 10^{-3} (\text{Wm}^{-1} \text{K}^{-1})$
$t$	Time	$(\text{s})$
$x$	Spatial distance (length of the reaction tube)	$(\text{m})$
$y$	Spatial distance (width of the reaction tube)	$(\text{m})$
$\alpha$	The fraction of fuel in the reaction-mixture at time $t = 0$	$(-)$
$\sigma$	A constant in the Gaussian profile for the initial condition	$\sigma = 0.15 (-)$
$\chi$	Heat transfer coefficient	$(\text{W m}^{-2} \text{K}^{-1})$

### 3.1. Model equations: one-dimensional problem

Temperature equation on  $0 \leq x \leq L$ :

$$k \frac{\partial^2 T}{\partial x^2} = C c_v \frac{\partial T}{\partial t} - Q A \exp\left[\frac{-E}{RT}\right] \mathcal{F} \mathcal{O}_2 + Q_i A_i \exp\left[\frac{-E_i}{RT}\right] \mathcal{F} + \chi \mathcal{G} (T - T_a). \quad (5)$$

Fuel equation on  $0 \leq x \leq L$ :

$$D_f \frac{\partial^2 \mathcal{F}}{\partial x^2} = \frac{\partial \mathcal{F}}{\partial t} + A \exp\left[\frac{-E}{RT}\right] \mathcal{F} \mathcal{O}_2 + A_i \exp\left[\frac{-E_i}{RT}\right] \mathcal{F}. \quad (6)$$

Oxygen equation on  $0 \leq x \leq L$ :

$$D_o \frac{\partial^2 \mathcal{O}_2}{\partial x^2} = \frac{\partial \mathcal{O}_2}{\partial t} + A \exp\left[\frac{-E}{RT}\right] \mathcal{F} \mathcal{O}_2. \quad (7)$$

Boundary conditions:

$$T(x=0) = T_a, \quad \left. \frac{\partial T}{\partial x} \right|_{x=L} = 0, \quad (8)$$

$$\left. \frac{\partial \mathcal{F}}{\partial x} \right|_{x=0} = 0, \quad \left. \frac{\partial \mathcal{F}}{\partial x} \right|_{x=L} = 0, \quad (9)$$

$$\left. \frac{\partial \mathcal{O}_2}{\partial x} \right|_{x=0} = 0, \quad \left. \frac{\partial \mathcal{O}_2}{\partial x} \right|_{x=L} = 0. \quad (10)$$

Initial conditions:

$$T(x, 0) = T_a + \frac{T}{1 - \exp[(-1)/(2\sigma^2)]} \left\{ \exp\left[-\frac{((x-L)/L)^2}{2\sigma^2}\right] - \exp\left[\frac{-1}{2\sigma^2}\right] \right\}, \quad (11)$$

$$\mathcal{F}(x, 0) = \alpha C, \quad (12)$$

$$\mathcal{O}_2(x, 0) = (1 - \alpha)C. \quad (13)$$

Equation (5) models the temperature of the reactor along its length. The term  $\chi \mathcal{G} (T - T_a)$  represents Newtonian cooling. We refer to the product  $\chi \mathcal{G}$  as the *effective heat transfer parameter*. Centre-manifold theory (and physical reasoning) gives the relationship between the geometric factor ( $\mathcal{G}$ ) and the half-thickness of the two-dimensional model ( $d$ ) as  $\mathcal{G} = 1/d$  [10]. The cases  $\chi \mathcal{G} = 0$  and  $\chi \mathcal{G} > 0$  represent a perfectly insulated reactor (an adiabatic reactor) and an imperfectly insulated reactor (a diabatic reactor), respectively. The former represents the infinite Biot number limit of a classical thermal explosion theory.

Equations (6) and (7) model the concentration of fuel and oxygen inside the reactor, respectively. For simplicity multi-component diffusion is not considered.

In equations (5)–(7) we have assumed that physical properties such as the thermal conductivity ( $k$ ), the volumetric heat-capacity ( $c_v$ ) and the diffusion coefficients ( $D_f$  and  $D_o$ ) are independent of the mixture composition.

In the boundary conditions, equations (8)–(10), we have assumed a no-flux boundary condition at  $x = L$  and at  $x = 0$  we have imposed a constant reactor temperature (infinite Biot number) and a no-flux condition for the reactants.

In the initial conditions, equations (11)–(13), we have assumed that the initial temperature decays in a Gaussian manner away from the centre of the reactor. At the edge of the reactor we have  $T(0, 0) = T_a$  and at the centre  $T(L, 0) = T_a + T$ . The initial concentration of the reactants is assumed to be uniform.

The system defined by equations (5)–(13) was integrated using the technique of the method of lines [13]. This is implemented in MATLAB using the routine ode15s which can handle differential algebraic equations of index 1 [14].

### 3.2. Model equations: two-dimensional problem

We reduce the integration domain by imposing a symmetry condition along the lines  $x = L$  and  $y = 0$ .

Temperature equation on  $0 \leq x \leq L, 0 \leq y \leq d$ :

$$k \left( \frac{\partial^2 T}{\partial x^2} + \frac{\partial^2 T}{\partial y^2} \right) = C c_v \frac{\partial T}{\partial t} - Q A \exp \left[ \frac{-E}{RT} \right] \mathcal{F} \mathcal{O}_2 + Q_i A_i \exp \left[ \frac{-E_i}{RT} \right] \mathcal{F}. \quad (14)$$

Fuel equation on  $0 \leq x \leq L, 0 \leq y \leq d$ :

$$D_f \left( \frac{\partial^2 \mathcal{F}}{\partial x^2} + \frac{\partial^2 \mathcal{F}}{\partial y^2} \right) = \frac{\partial \mathcal{F}}{\partial t} + A \exp \left[ \frac{-E}{RT} \right] \mathcal{F} \mathcal{O}_2 + A_i \exp \left[ \frac{-E_i}{RT} \right] \mathcal{F}. \quad (15)$$

Oxygen equation on  $0 \leq x \leq L, 0 \leq y \leq d$ :

$$D_o \left( \frac{\partial^2 \mathcal{O}_2}{\partial x^2} + \frac{\partial^2 \mathcal{O}_2}{\partial y^2} \right) = \frac{\partial \mathcal{O}_2}{\partial t} + A \exp \left[ \frac{-E}{RT} \right] \mathcal{F} \mathcal{O}_2. \quad (16)$$

Boundary conditions along  $x = 0$ :

$$T(0, y) = T_a, \quad \left. \frac{\partial \mathcal{F}}{\partial x} \right|_{0,y} = 0, \quad \left. \frac{\partial \mathcal{O}_2}{\partial x} \right|_{0,y} = 0. \quad (17)$$

Boundary conditions along  $x = L$ :

$$\left. \frac{\partial T}{\partial x} \right|_{L,y} = 0, \quad \left. \frac{\partial \mathcal{F}}{\partial x} \right|_{L,y} = 0, \quad \left. \frac{\partial \mathcal{O}_2}{\partial x} \right|_{L,y} = 0. \quad (18)$$

Boundary conditions along  $y = 0$ :

$$\left. \frac{\partial T}{\partial y} \right|_{x,0} = 0, \quad \left. \frac{\partial \mathcal{F}}{\partial y} \right|_{x,0} = 0, \quad \left. \frac{\partial \mathcal{O}_2}{\partial y} \right|_{x,0} = 0. \quad (19)$$

Boundary conditions along  $y = d$ :

$$-k \left. \frac{\partial T}{\partial x} \right|_{x,d} = \chi (T - T_a), \quad \left. \frac{\partial \mathcal{O}_2}{\partial y} \right|_{x,d} = 0, \quad \left. \frac{\partial \mathcal{O}_2}{\partial y} \right|_{x,d} = 0. \quad (20)$$

Initial conditions:

$$T(x, 0) = T_a + \frac{T}{1 - \exp[(-1)/(2\sigma^2)]} \left\{ \exp\left[\frac{-((x-L)/L)^2}{2\sigma^2}\right] - \exp\left[\frac{-1}{2\sigma^2}\right] \right\}, \quad (21)$$

$$\mathcal{F}(x, 0) = \alpha C, \quad (22)$$

$$\mathcal{O}_2(x, 0) = (1 - \alpha)C. \quad (23)$$

In the two-dimensional model the energy equation (14) no longer contains a Newtonian cooling term. This now appears in the temperature boundary condition at  $y = d$ , equation (20).

The system defined by equations (14)–(23) was integrated using FlexPDE [15] which uses the finite element method to solve boundary value problems. Its features include adaptive grid refinement (eliminating the need to determine an appropriate mesh) and adaptive time stepping (based on the user's pre-determined accuracy).

In order to compare the results of the one- and two-dimensional models we calculate an effective heat-transfer parameter for the two-dimensional model by dividing the heat-transfer coefficient ( $\chi$ ) by the half-width of the reactor ( $d$ ) [10].

### 3.3. Characterising the performance of the reactor

In investigating the properties of the system defined by equations (5)–(13) we are primarily interested in distinguishing between regions of super-criticality, representing combustion, and sub-criticality, corresponding to acquiescence of the reactants. To do this we use two indicators of the behaviour of the system: the *maximum temperature increase* ( $\Delta T_{\max}$ ) and the *fractional conversion* at 20 seconds ( $\mathcal{F}_C$ ).

We define the maximum temperature increase by

$$\Delta T_{\max} = \max_t \max_{0 \leq x \leq L} (T(x, t) - T(x, 0)). \quad (24)$$

Note that  $\Delta T_{\max}$  is non-zero in the absence of chemical reaction ( $\alpha = 0$  and  $\alpha = 1$ ) – due to diffusion of the energy deposited in the initial temperature profile through the reactor. Other choices to measure the temperature rise within the reactor are possible.

We define the fractional conversion by

$$\mathcal{F}_C = \frac{\alpha C - \int_{x=0}^{x=L} \mathcal{F}(x, t = 20) dx}{\alpha C}. \quad (25)$$

In practice we do not need to integrate the fuel concentration over the reactor domain because numerical investigations reveal that (in most cases) by  $t = 20$  the concentration profile is flat.

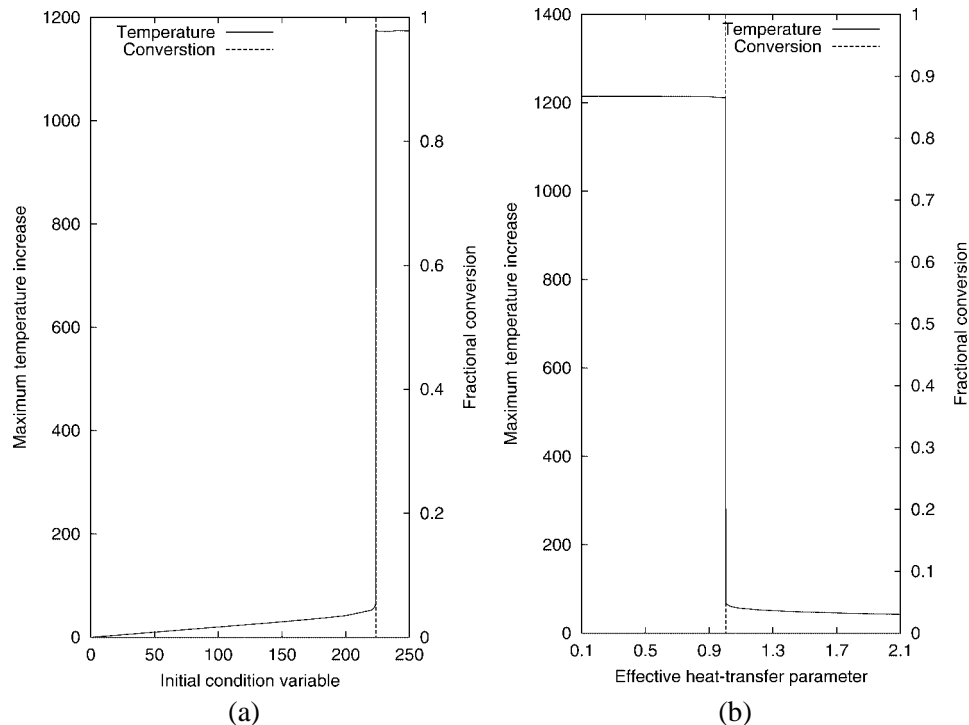


Figure 1. Criticality in the adiabatic and diabatic one-dimensional reactors. (a) Adiabatic one-dimensional reactor. (b) Diabatic one-dimensional reactor. Parameter values: (a)  $\alpha = 0.5$  and  $\chi\mathcal{G} = 0 \text{ W K}^{-1} \text{ m}^{-3}$ , (b)  $\alpha = 0.45$  and  $\mathcal{T} = 226 \text{ K}$ .

## 4. Results

In section 4.1 we describe the process by which flammability limits are determined for both of our models. Flammability limits for the two models are compared in section 4.2.

### 4.1. Determination of criticality

Flammability limits are determined experimentally under fixed ignition conditions, for example, by applying a flame for a specified length of time to the reaction mixture or using a particular type of spark igniter. In our model this is equivalent to specifying the value of the initial condition variable ( $\mathcal{T}$ ).

Figure 1(a) shows how the response of the system depends upon the value of the initial condition variable ( $\mathcal{T}$ ), or equivalently how “strong” the ignition source is. This is for a one-dimensional adiabatic reactor with equal-molar initial concentrations of fuel and oxygen. For subcritical values of  $\mathcal{T}$  the fractional conversion is zero and there is a small temperature increase. As noted in section 3.3 the non-zero temperature increase is primarily caused by diffusion of the energy placed into the reactor at time  $t = 0$  by the ignition source. For sufficiently large values of  $\mathcal{T}$  the fractional conversion is one

and the maximum temperature increase is high. The regions of sub- and super-criticality are clearly demarcated. We define the critical value of  $\mathcal{T}$  as the lowest value at which ignition occurs. For figure 1(a) this value is  $\mathcal{T} = 223.7$  K. The critical value of the initial condition variable will be higher for other values of the fuel fraction. The critical value would also be higher for a given value of the heat-transfer coefficient in a diabatic reactor.

In the remainder of this paper we fix the “strength” of the ignition source and investigate how the transition from sub- to super-criticality depends upon the values of the effective heat-transfer parameter and the fuel fraction (flammability limits). We consider the cases  $\mathcal{T} = 226$  K and  $\mathcal{T} = 246$  K. The former represents an ignition source that is close to criticality for the adiabatic reactor when  $\alpha = 0.5$ , the latter represents a stronger ignition source. Note that as we are now interested in behaviour in a diabatic reactor the ignition source has to be stronger than the critical value in the adiabatic reactor.

Figure 1(b) illustrates the transition from super- to sub-critical behaviour as the effective heat-transfer parameter is increased. In the supercritical region the fractional conversion is one and there is a high maximum temperature increase. In the subcritical region the fractional conversion is zero and there is a low maximum temperature increase. The existence of a critical value of the effective heat-transfer parameter is evident and the use of sensitivity analysis to identify criticality is not needed here, unlike in some cases of our previous investigation [2]. We define the critical value of the effective heat-transfer parameter to be the highest value at which ignition occurs. Consequently the reaction mixture specified by  $\alpha = 0.45$  is flammable if  $0 \leq \chi\mathcal{G} \leq 1.00$  when  $\mathcal{T} = 226$  K. Furthermore, figure 1(b) shows that the critical value of the effective heat-transfer parameter is independent of the choice of our indicator functions (maximum temperature and fractional conversion).

#### 4.2. Comparison of flammability limits in the one- and two-dimensional models

The process illustrated in figure 1(b) was repeated for various values of the fuel fraction and for two values of the initial condition variable. These calculations were made for both the one- and two-dimensional model. The dependence of the flammability limits upon the effective heat-transfer parameter ( $\chi\mathcal{G}$ ) is shown in figure 2. In both diagrams flammability limits are only shown for  $\alpha \leq 0.5$  because the flammability limits are symmetric in  $\alpha$  about the value 0.5.

Note that the fuel fraction ( $\alpha$ ) only appears in equations (12)–(13) and that when  $A_i = 0$  our model does not differentiate between the fuel and oxygen species. Thus in our previous paper [2], where the oxidation mechanism only included reaction (3), the behaviour of the model, i.e., flammability limits, was anticipated to be symmetric in the fuel fraction around the point  $\alpha = 0.5$ . However, when  $A_i > 0$  there is a distinction between the fuel and oxygen species and the model is no longer symmetric with respect to the fuel fraction variable. The unexpected symmetry in figure 2 occurs because reaction (4) is a high-temperature reaction that is negligible at the temperatures



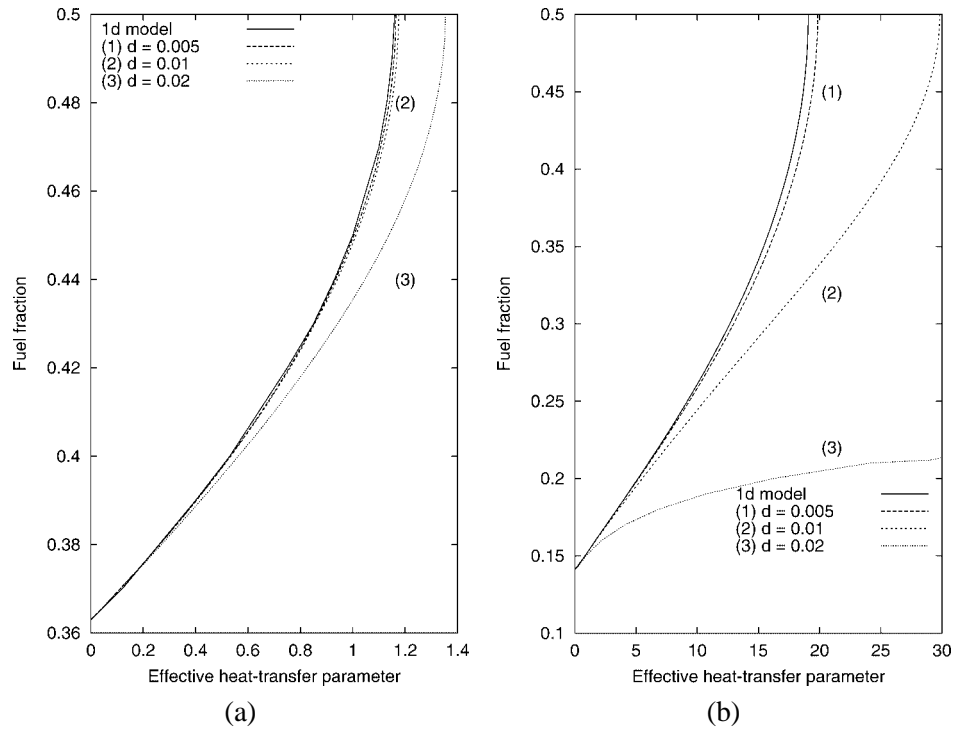


Figure 2. Comparison of flammability limits calculated in the one- and two-dimensional models. (a) Initial condition variable  $T = 226$  K. (b) Initial condition variable  $T = 246$  K. Points to the left of a particular curve are flammable, whereas points to the right are non-flammable.

at which ignition occurs. Consequently the conditions for ignition are only dependent upon reaction (3).

Figure 2 clearly shows that the one-dimensional model is a lower-bound for the two-dimensional model. In figure 2(a) the one-dimensional model is seen to be a good approximation for the two-dimensional model when  $d \leq 0.01$  m. When the half-width is increased to  $d = 0.02$  m the one-dimensional model mimics the general trend of the two-dimensional model. However, the accuracy of the one-dimensional approximation decreases as the fuel fraction increases. In the worst case ( $\alpha = 0.5$ ) the critical value of the effective heat-transfer parameter in the two-dimensional model is approximately 17% larger than the value predicted by the reduced model. In figure 2(b) the initial condition variable has been increased to  $T = 246$  K. When the half-width is  $d = 0.005$  and  $d = 0.01$  the one-dimensional model predicts the general trends seen in the two-dimensional model. In the worst case ( $\alpha = 0.5$ ) the critical value of the effective heat-transfer parameter in the two-dimensional model is approximately 3.9% higher ( $d = 0.005$ ) and 36% higher ( $d = 0.01$ ) than that predicted by the reduced model. The one-dimensional approximation is clearly inadequate for a half-width  $d = 0.02$  m.

## 5. Discussion

Flammability limits are usually measured in the US Bureau of Mines apparatus [16]. In this method an ignition source is introduced at the lower end of a vertical tube of length 1.5 m and a mixture deemed to be flammable if a flame can propagate at least half-way up the tube. Conceptually, one imagines the flame as being a wave. For supercritical systems we have observed waves travelling across our “tube”. These are similar in structure to those reported elsewhere [17]. Consequently, spatial profiles are not presented here.

## 6. Conclusion

In this paper we have compared flammability limits of fuel–oxygen mixtures in a two-dimensional slab to the corresponding one-dimensional approximation which incorporates an averaged heat-loss term. We used a simple chemical mechanism consisting of a single exothermic reaction, an oxidation step, and a single endothermic reaction, representing “incomplete combustion reactions”. For the parameter values used in this paper there was a clear-cut distinction between sub- and super-critical behaviour.

The accuracy of the one-dimensional model decreases as either the half-thickness of the tube is increased or the strength of the ignition source, represented by initial condition variable, is increased. For a value of the initial condition variable  $\mathcal{T} = 226$  K just above the minimum ignition strength required to ignite an equal-molar fuel–oxygen mixture in an adiabatic reactor ( $\mathcal{T} = 223.7$  K), the one-dimensional model accurately reproduced the results of the two-dimensional model for values of the half-thickness  $d \leq 0.01$  m and provided a reasonable approximation when  $d = 0.02$  m. For a slightly higher value of the initial condition variable ( $\mathcal{T} = 246$  K) the one-dimensional model was only accurate for  $d \leq 0.005$  m. For sufficiently thick tubes the one-dimensional model was shown to be inadequate at predicting the behaviour of the two-dimensional model (see curve 3 in figure 2(b)). Thus the reduced model has only a very limited range of applicability.

An interesting question that remains unanswered is whether the one-dimensional model becomes more robust if a more realistic low-temperature ignition mechanism is used.

## Acknowledgments

The authors would like to thank Dr. G.N. Mercer and Dr. R.O. Weber (both School of Mathematics and Statistics, ADFA) for helpful discussions.

During this work M.I. Nelson was supported by a grant from the the Australian Research Council at ADFA.

**References**

- [1] D. Drysdale, *An Introduction to Fire Dynamics* (Wiley, New York, 1999).
- [2] M.I. Nelson and H.S. Sidhu, Flammability limits of an oxidation reaction in a batch reactor, Preprint (2003).
- [3] A. Búcsi and J. Rychlý, *Poly. Degrad. Stab.* 38 (1992) 33.
- [4] J. Rychlý and L. Costa, *Fire Mater.* 19 (1995) 215.
- [5] J. Rychlý and L. Rychlá, *Fire Mater.* 10 (1986) 7.
- [6] J. Rychlý and L. Rychlá, *Poly. Degrad. Stab.* 54 (1996) 249.
- [7] J. Billingham and G.N. Mercer, *Combust. Theor. Model.* 5 (2001) 319.
- [8] G.N. Mercer, R.O. Weber and H.S. Sidhu, *Proc. Roy. Soc. London Ser. A* 454 (1998) 2015.
- [9] G.N. Mercer and R.O. Weber, *Proc. Roy. Soc. London Ser. A* 450 (1995) 193.
- [10] G.N. Mercer and R.O. Weber, *Combust. Theor. Model.* 1 (1997) 157.
- [11] G.N. Mercer and R.O. Weber, *Proc. Roy. Soc. London Ser. A* 453 (1997) 1543.
- [12] R.O. Weber and S.D. Watt, *J. Austral. Math. Soc. Ser. B* 38 (1997) 464.
- [13] W.E. Schiesser, *The Numerical Method of Lines: Integration of Partial Differential Equations* (Academic Press, New York, 1991).
- [14] L.F. Shampine, M.W. Reichelt and J.A. Kierzenka, *SIAM Review* 41 (1999) 538.
- [15] PDESolutions Inc., FlexPDE<sup>tm</sup>, finite element software, <http://www.pdesolutions.com>
- [16] H.F. Coward and G.W. Jones, *Bulletin – United States Bureau of Mines* (1952) 503.
- [17] M.J. Sexton, H.S. Sidhu and M.I. Nelson, *The ANZIAM Journal* 44(E) (2003) C687.